Sympatric speciation revealed by genome-wide divergence in the blind mole rat *Spalax*

Kexin Li[a,b,1], Wei Hong[a,1], Hengwu Jiao[a], Guo-Dong Wang[c], Karl A. Rodriguez[d,e], Rochelle Buffenstein[d,e,f], Yang Zhao[b], Eviatar Nevo[b,2], and Huabin Zhao[a,2]

[a]Department of Ecology, College of Life Sciences, Wuhan University, Wuhan 430072, China; [b]Institute of Evolution, University of Haifa, Haifa 3498838, Israel; [c]State Key Laboratory of Genetic Resources and Evolution, Kunming Institute of Zoology, Chinese Academy of Sciences, Kunming 650223, China; [d]Sam and Anne Barshop Center for Longevity and Aging Studies, University of Texas Health Science Center at San Antonio, San Antonio, TX 78229; [e]Department of Physiology, University of Texas Health Science Center at San Antonio, San Antonio, TX 78229; and [f]Calico, South San Francisco, CA 94080

Contributed by Eviatar Nevo, July 29, 2015 (sent for review July 6, 2015; reviewed by Francisco J. Ayala, Sergey Gavrilets, and Alan Robert Templeton)

Sympatric speciation (SS), i.e., speciation within a freely breeding population or in contiguous populations, was first proposed by Darwin [Darwin C (1859) *On the Origins of Species by Means of Natural Selection*] and is still controversial despite theoretical support [Gavrilets S (2004) *Fitness Landscapes and the Origin of Species (MPB-41)*] and mounting empirical evidence. Speciation of subterranean mammals generally, including the genus *Spalax*, was considered hitherto allopatric, whereby new species arise primarily through geographic isolation. Here we show in *Spalax* a case of genome-wide divergence analysis in mammals, demonstrating that SS in continuous populations, with gene flow, encompasses multiple widespread genomic adaptive complexes, associated with the sharply divergent ecologies. The two abutting soil populations of *S. galili* in northern Israel habituate the ancestral Senonian chalk population and abutting derivative Plio-Pleistocene basalt population. Population divergence originated ∼0.2–0.4 Mya based on both nuclear and mitochondrial genome analyses. Population structure analysis displayed two distinctly divergent clusters of chalk and basalt populations. Natural selection has acted on 300+ genes across the genome, diverging *Spalax* chalk and basalt soil populations. Gene ontology enrichment analysis highlights strong but differential soil population adaptive complexes: in basalt, sensory perception, musculature, metabolism, and energetics, and in chalk, nutrition and neurogenetics are outstanding. Population differentiation of chemoreceptor genes suggests intersoil population's mate and habitat choice substantiating SS. Importantly, distinctions in protein degradation may also contribute to SS. Natural selection and natural genetic engineering [Shapiro JA (2011) *Evolution: A View From the 21st Century*] overrule gene flow, evolving divergent ecological adaptive complexes. Sharp ecological divergences abound in nature; therefore, SS appears to be an important mode of speciation as first envisaged by Darwin [Darwin C (1859) *On the Origins of Species by Means of Natural Selection*].

sympatric speciation | population genetics | genome divergence | ecological adaptation | natural selection

Despite more than a century since first proposed by Darwin (1), the concept of sympatric speciation (SS) as a major mode of speciation, i.e., formation of new species within a freely breeding population with ongoing gene flow, is still highly controversial and evaluated both skeptically and critically (2). Interestingly, recent empirical studies (*SI Appendix*) and theoretical assessments (3) support SS. Claims of SS must demonstrate species sympatry, sister relationship, reproductive isolation, and that an earlier allopatric phase is highly unlikely (2). We recently described two studies of SS in two evolutionarily divergent mammals, the blind subterranean mole rat *Spalax galili* (4) (Fig. 1 *A*–*C*) and the spiny mice, *Acomys*, at "Evolution Canyon" (EC), Mount Carmel, Israel (5). Moreover, the Evolution Canyon microsite in Israel has been suggested as a cradle for SS across life, based on incipient SS of five distant taxons: bacteria, wild barley, fruit flies, beetles, and spiny mice (6). Importantly, only a few studies to date have investigated whole genome evolution in an attempt to uncover genome architectural changes during SS (7). Here we show that SS in *S. galili* encompasses extensive adaptive complexes across the genome associated with the sharply abutting and divergent chalk and basalt ecologies where SS took place, i.e., in sympatry and not in an earlier allopatry (4).

Results

Population Sequencing and Variation Calling. Five individuals of the blind mole rat (*S. galili*) from the chalk rendzina soil and six from the abutting basalt soil (Fig. 1 *A*–*C*) were collected for genome sequencing. Of the 11 animals, the generated data for each individual, which had a genome size of ∼3G bp (8), ranged from 19.6 to 30.8 Gb, corresponding to sequencing depths of 6.36×–10× (Table S1). A total of 14,539,199 SNPs were identified, with 3,717,338 and 3,361,317 SNPs unique to the basalt and chalk populations, respectively (Fig. S1). We validated our SNP calling strategy with traditional Sanger sequencing technology and found that the genome-wide false-positive rate is less than 6% and the false-negative rate is less than 13% (*SI Materials and Methods*).

Significance

Sympatric speciation is still highly controversial. Here we demonstrate, based on genome-wide divergence analysis, that sympatric speciation in the blind subterranean rodent *Spalax galili* encompasses multiple and widespread genomic adaptive complexes associated with the sharply divergent and abutting basalt and chalk soil populations. Gene ontology enrichment analysis highlights sensory perception, musculature, metabolism, and energetics in basalt against neurogenetics and nutrition in chalk. Population divergence of chemoreceptor genes suggests the operation of mate and habitat choices, substantiating sympatric speciation. Natural selection and natural genetic engineering overrule gene flow, evolving divergent ecological adaptive complexes. Sympatric speciation may be a common speciation mode, as envisaged by Darwin, due to the abundance of sharp divergent geological, edaphic, climatic, and biotic ecologies in nature.

Author contributions: K.L., R.B., E.N., and H.Z. designed research; K.L., W.H., H.J., K.A.R., and Y.Z. performed research; W.H., H.J., G.-D.W., E.N., and H.Z. analyzed data; and K.L., W.H., H.J., K.A.R., E.N., and H.Z. wrote the paper.

Reviewers: F.J.A., University of California, Irvine; S.G., University of Tennessee; and A.R.T., Washington University at St. Louis.

The authors declare no conflict of interest.

Data deposition: The sequence reported in this paper has been deposited in the GenBank database (accession nos. SRP058797 and KT009027–KT012480).

[1]K.L. and W.H. contributed equally to this work.

[2]To whom correspondence may be addressed. Email: nevo@research.haifa.ac.il or huabinzhao@whu.edu.cn.

This article contains supporting information online at www.pnas.org/lookup/suppl/doi:10.1073/pnas.1514896112/-/DCSupplemental.

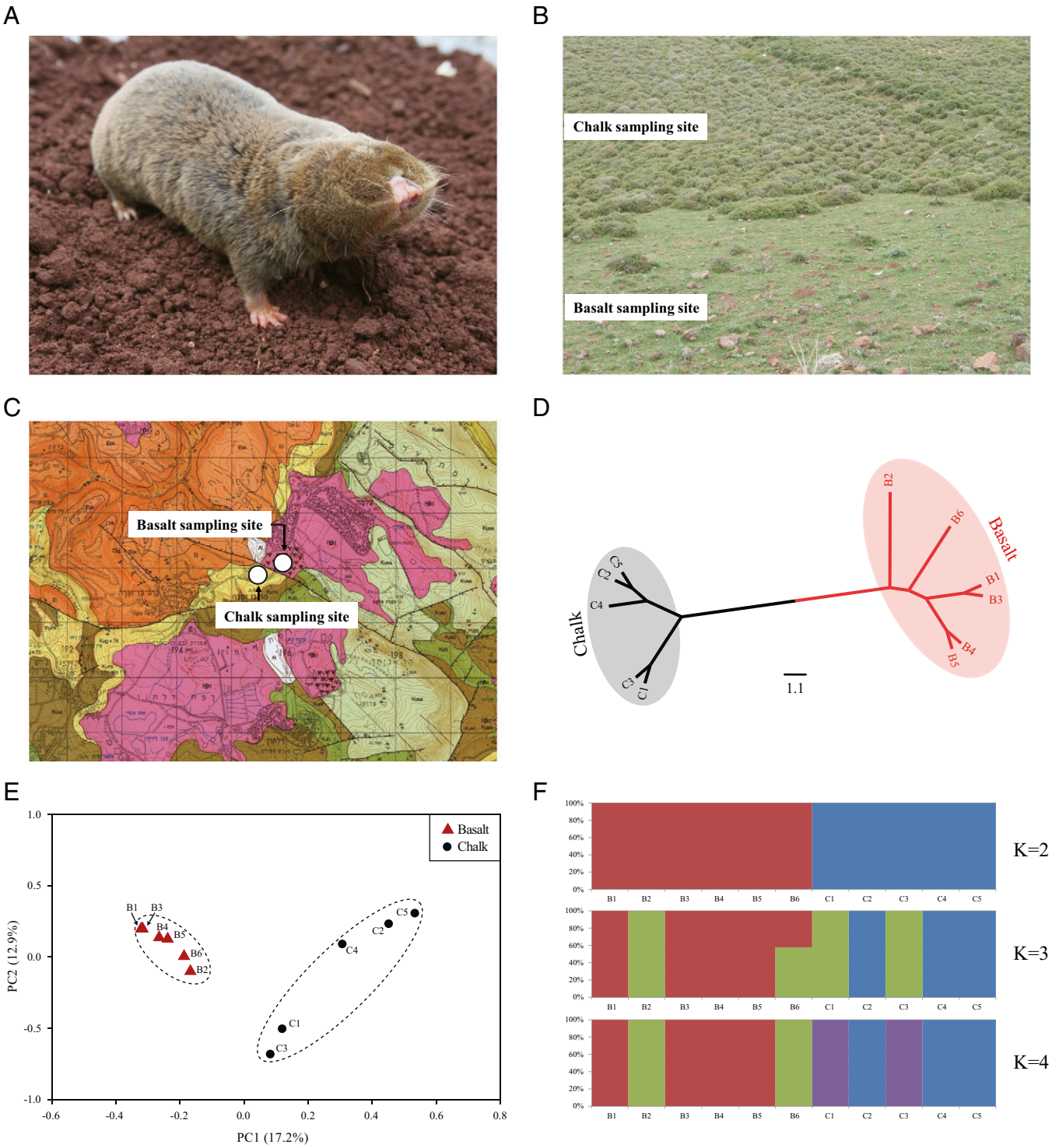

Fig. 1. Study subject, ecological, and genomic divergence in sympatric speciation. (*A*) The blind mole rat, *S. galili*. (*B*) Vegetation formation exposed with mounds in basalt and covered by dense bushes of *Sarcoptherium spinosum* in chalk. (*C*) Geological map. Chalk is in yellow and basalt is in pink, separated by a geological fault. (*D*) NJ tree based on all of the SNPs. Red, basalt individuals; black, chalk individuals. (*E*) PCA of two *Spalax* soil populations. Red triangles, basalt individuals; black circles, chalk individuals. (*F*) Population genetic structure of two *Spalax* soil populations when K = 2, 3, and 4.

Genetic Diversity and Structure of the Two Populations. Whole genome genetic diversity, estimated by Watterson's θ for each individual, was significantly higher in chalk (mean $\theta = 1.13 \times 10^{-3}$) than in basalt ($1.09 \times 10^{-3}$; $P < 2.2 \times 10^{-16}$, Mann–Whitney U test). Two distinct soil population clusters, basalt and chalk, were identified by the neighbor-joining (NJ) method (Fig. 1*D*) and by principal component analysis (PCA) (Fig. 1*E*) based on all SNPs. In PCA, the first and second component explained 17.2% and 12.9% of the genetic differences, respectively. A maximum likelihood analysis of population structure was undertaken based on K = 2, 3, and 4 (Fig. 1*F*). With K = 2, the basalt population is completely separated from the chalk population. In clustering by

K = 3, both populations were divided into further subgroups but with the same genetic background (in green), notably, the individual B6 spans both chalk and basalt populations, possibly a recombinant individual. With K = 4, both populations were split into two subgroups, respectively (Fig. 1*F*).

Linkage Disequilibrium and Population Demography. Linkage disequilibrium (LD), measured by the correlation coefficient (r^2), decreased rapidly below 0.2 within 1,000 bp in both populations (Fig. 2*A*). Mean population recombination rate per kilobase ($\rho = 4Ne \times r$) in basalt was 1.515, significantly higher than in chalk of 1.125 ($P < 2.2 \times 10^{-16}$, Mann–Whitney *U* test). Estimated extant effective population size (*Ne*) for chalk and basalt was 72,380 and 116,800, respectively, and the inferred ancestral *Ne* was 84,570 (Fig. 2*B*). The migration rates of chalk to basalt and basalt to chalk were 1.788 and 5.809 per generation (Fig. 2*B*), respectively. The two *Spalax galili* soil populations were estimated to split ~0.2–0.4 Mya based on both whole genome and mitochondrial genome analyses (Fig. 2*B* and *SI Materials and Methods*).

Population Genomic Divergence and Functional Enrichment. Putatively selected genes (PSGs) were identified by screening genomic regions that show low diversity (measured by Tajima' *D*) in one population but high divergence [measured by fixation index (F_{ST})] between the two populations. A total of 128 genes in the basalt population and 189 genes in the chalk population were identified with the strongest signature of positive selection (Tables S2 and S3). Gene ontology (GO) enrichment analysis revealed functions of musculature, energetics, metabolism, and sensory biology (Fig. 3) distinguished in basalt. In contrast, functions related to neurogenetics and nutrition were enriched in the chalk population (Fig. 3). Our genome-wide scans for positive selection highlight how, where, and why adaptive evolution has shaped genetic variations.

We sequenced 22 olfactory receptor (*OR*) genes (i.e., genes are numbered in Table 1) (Fig. S2), 20 bitter taste receptor (*Tas2r*) genes (Fig. S3), and 18 putatively neutral noncoding regions (*NCs*). Specifically, *ORs* refer to a group of olfactory receptor genes; *Tas2rs* refer to a group of type 2 taste receptor genes; *NCs* refer to a group of neutral noncoding regions. Pairwise F_{ST} estimates revealed that 10 *OR*s, 9 *Tas2r*s, and 1 neutral region are significantly differentiated between the chalk and basalt populations [$P < 0.05$ after false discovery rate (FDR) adjustment; Table 1]. The rate of significantly differentiated loci is statistically higher in *ORs* (10/22 = 45.5%) than in *NCs* (1/18 = 5.6%) ($P = 0.011$, two-tailed Fisher exact test), and the same is true for *Tas2r*s ($P = 0.009$).

Differences in Proteostasis of the Two Populations. Besides genomics, proteomics, particularly mechanisms regulating proteostasis, selectively drive soil population divergence. Mesic basalt population has a threefold significantly greater proteasome chymotrypsin-like activity in muscle and twofold higher trypsin-like and caspase-like activities than the chalk population (Fig. 4*A*) based on analyses of seven animals from each population. The basalt population displayed significantly higher α7 levels (Fig. 4*B*) than the chalk population, suggesting higher numbers of proteasomes in these tissues facilitating enhanced degradation of damaged or misfolded proteins through this protein degradation machinery. In contrast, the chalk population showed significantly higher levels of ATG7 and autophagic flux (LC3II/LC3I ratio) (Fig. 4*C*). This protein degradation profile suggested more of a reliance on autophagy in chalk population.

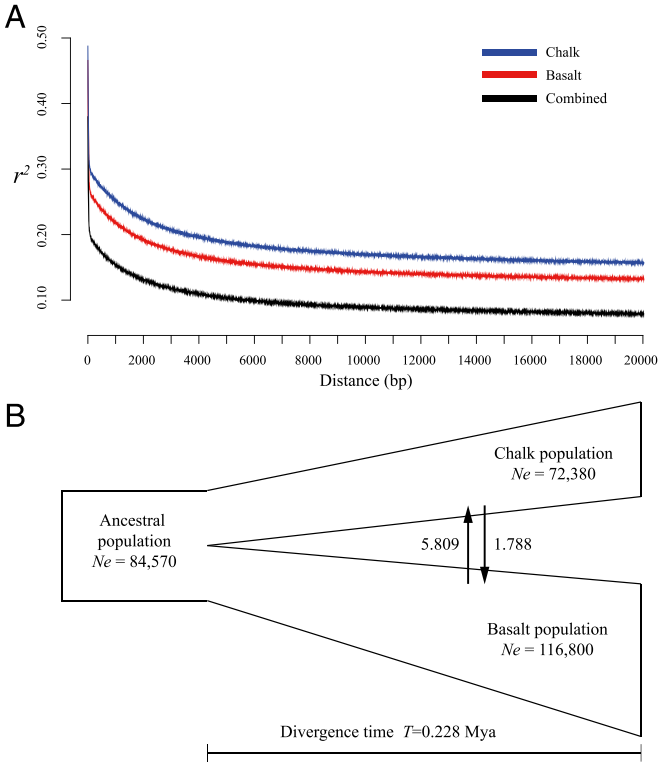

Fig. 2. LD and demographic structure. (*A*) LD decay of two continuous *S. galili* populations. *x* axis stands for physical distances (bp), whereas *y* axis stands for r^2. (*B*) Inferred demographic history for the two abutting soil populations (chalk vs. basalt) of *S. galili*. The extant and ancestral population sizes (*Ne*) of the chalk and basalt populations are indicated, and the migration rates between the two populations are provided. The divergence time (*T*) between two populations was inferred.

Discussion

Genetic Diversity, Population Structure, Speciation Genes, and Reproductive Isolation. Genetic diversity at the local chalk-basalt state parallels the regional patterns (9, 10). The basalt and chalk mole rat populations were grouped separately (Fig. 1 *D–F*), suggesting genome-wide divergence of the two abutting soil populations. Population structure analysis showed similar clustering as revealed by mtDNA (4). The B6 individual showed a genetic mixture of both the chalk and basalt populations, which may indicate some limited gene flow, as was shown earlier by a recombinant individual in the interface of chalk and basalt (4) and a mound row extending from basalt to chalk was also observed in the field. Remarkably, genetic diversity from whole genome analysis is consistent with earlier estimates by mtDNA (4) and AFLP (11), where genetic polymorphism was significantly higher in chalk than in basalt. This finding supports earlier evidence that genetic diversity is possibly associated with a more stressed environment (5, 6, 9, 10). We deduced, across the whole genome, positively selected speciation genes (SGs). We hypothesize that besides highlighting strong selection, additional factors could potentially contribute directly or indirectly to reproductive isolation (RI) in abutting *Spalax* soil populations associated with SS (Table S4). These factors include habitat selection, chemoreceptor divergence, and preliminary indications of mate choice.

LD and Population Demography. Rapid LD decay indicates high recombination rates or large effective population sizes (12). LD level is relatively lower in basalt than in the chalk population, possibly because of the larger basalt population size (4) (Fig. 2*B*) and the higher temperature stress in chalk as was shown experimentally in *Drosophila* (13). *Ne* of chalk is smaller than that of basalt (4) (Fig. 2*B*), probably due to lower food resources (14). The larger *Ne* of the basalt population (Fig. 2*B*) is similar to current population estimates (14). The recombination rate is significantly

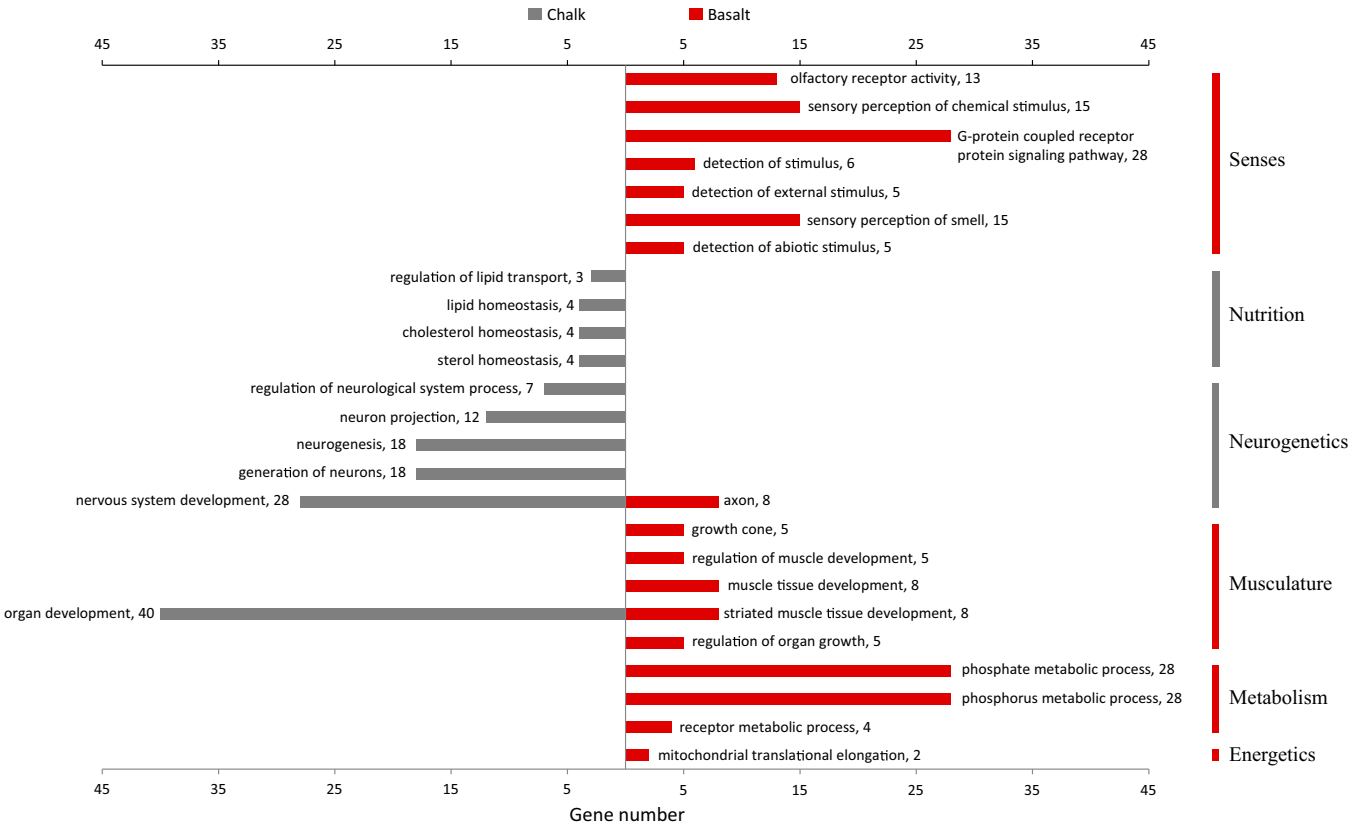

Fig. 3. GO enrichment analysis of putatively selected genes in chalk and basalt *S. galili* populations. Gene number is provided next to each GO term.

higher in basalt than that in chalk possibly due to adaptation to the novel basalt niche (15). The combined lower LD may suggest that LDs are soil specifically selected for the chalk and basalt separately rather than generally for both. There are more animals migrating from basalt to chalk populations possibly because of the higher population density in basalt.

Functional Adaptive Complexes. Functional enrichment analysis of GO terms revealed the remarkable divergence of biological differences between the abutting *Spalax* soil populations, indicating genome-wide adaptive complexes in each soil population resulting from its soil-unique, multiple-specific ecological stresses. Burrow digging, a major activity of mole rats, is harder

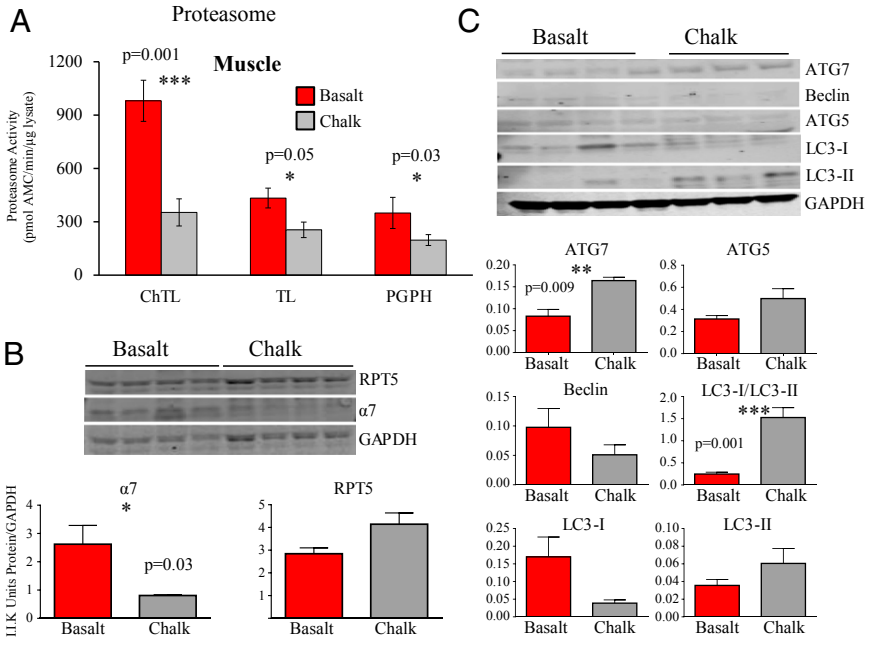

Fig. 4. Differences in the proteolytic machinery of *Spalax galili* basalt and chalk populations. (*A*) 20S proteasome activity measured by degradation of optimized peptides cleaved by the three active sites, chymotrypsin-like (ChTL), trypsin-like (TL), and post-glutamyl, peptide hydrolyzing (PGPH) or caspase-like, show higher levels of activity in the basalt population. (*B*) Higher levels of the constitutive 20S proteasome subunit α7 support the observation of the increase in activity in basalt population. (*C*) The chalk population protein degradation profile suggests more of a reliance on autophagy, with significantly higher levels of ATG7 and autophagic flux (LC3II/LC3I ratio).

Table 1. Pairwise F_{ST} statistics of olfactory receptor genes (*OR1-OR22*), bitter taste receptor genes (*Tas2r1-Tas2r20*), and putatively neutral noncoding regions (*NC1-NC18*) between basalt and chalk populations

Loci	F_{ST}	FDR
OR1	0.074	0.093
OR2	0.055	<u>0.029</u>
OR3	0.037	0.051
OR4	0.061	<u>0.011</u>
OR5	0.320	<u>0.000</u>
OR6	0.106	<u>0.029</u>
OR7	0.023	0.465
OR8	0.029	0.093
OR9	0.040	0.220
OR10	0.064	0.188
OR11	−0.003	0.663
OR12	0.000	0.220
OR13	−0.004	0.051
OR14	0.120	<u>0.033</u>
OR15	0.107	<u>0.040</u>
OR16	0.007	<u>0.037</u>
OR17	0.040	<u>0.029</u>
OR18	0.049	0.208
OR19	0.008	<u>0.029</u>
OR20	0.014	<u>0.042</u>
OR21	−0.006	0.155
OR22	0.050	0.169
Tas2r1	−0.025	0.752
Tas2r2	−0.014	0.354
Tas2r3	0.045	<u>0.016</u>
Tas2r4	0.023	0.297
Tas2r5	−0.018	0.604
Tas2r6	−0.001	0.072
Tas2r7	0.000	0.109
Tas2r8	0.000	0.752
Tas2r9	0.015	0.157
Tas2r10	0.166	<u>0.026</u>
Tas2r11	0.104	<u>0.047</u>
Tas2r12	−0.013	0.540
Tas2r13	0.052	<u>0.035</u>
Tas2r14	0.005	0.467
Tas2r15	0.130	<u>0.023</u>
Tas2r16	0.127	<u>0.000</u>
Tas2r17	0.320	<u>0.000</u>
Tas2r18	−0.004	0.516
Tas2r19	0.056	<u>0.000</u>
Tas2r20	0.080	<u>0.016</u>
NC1	0.014	0.458
NC2	−0.008	0.418
NC3	0.037	0.144
NC4	0.056	0.268
NC5	0.064	0.413
NC6	0.061	0.063
NC7	0.042	0.261
NC8	0.005	0.694
NC9	0.050	0.153
NC10	0.002	0.413
NC11	−0.035	0.939
NC12	0.064	0.261
NC13	0.030	0.153
NC14	0.021	<u>0.018</u>
NC15	0.018	0.371
NC16	0.017	0.153
NC17	−0.011	0.413
NC18	−0.009	0.458

Significant *P* values are underlined. The genes and noncoding regions were numbered in arbitrary order. FDR, false discovery rate; F_{ST} is the fixation index.

in compact basalt than in loose chalk (4), evidenced by several GO terms such as musculature, energetics, and sensory biology (Fig. 3). Accordingly, activity patterns (4) and mound density (14) are significantly higher in basalt than in chalk. Remarkably, the clay-rich basalt is harder and sticky, requiring more energy in digging. The enriched metabolic PSGs in basalt reflect the higher resting metabolic rate (RMR) in basalt than in chalk mole rats (4), as is true regionally in northern *S. galili* compared with southern *S. judaei* due to low food resources in the latter (16). Olfaction, developed in *Spalax* (17), is under stronger selection in basalt than in the chalk population, possibly due to higher food diversity and chemical resources in basalt. Likewise, soil moisture is higher in basalt than in chalk (14), increasing odor saturability in the soil and enhancing olfactory reception (18, 19). Finally, sensory perception of chemical stimuli may increase during the colonization of the chalk ancestors into the novel basalt niche (20) due to the higher level of selective pressure for mate choice.

This local pattern of neurogenetics and nutrition parallels the regional one of *S. judaei,* characterized by high genetic diversity (21), limited food resources, and relatively bigger brain size (22). Both locally (chalk population of *S. galili*) and regionally (*S. judaei*), food resources are limited; hence, larger territories and magnetic orientation from the nest to the periphery influence selection for advanced neurogenetics (22) (Fig. 3). Local and regional parallel patterns highlight the adaptive nature of the above traits.

Genetic variations in olfactory and taste receptors may underlie both mate and habitat choice in speciation (23). The divergence of both olfactory and taste receptor genes strongly suggest that olfaction and taste have undergone diversifying selection in population divergence and premating reproductive isolation. Thus, chemosensory habitat and mate preferences may substantiate SS in the blind mole rats.

Greater digging in harder basalt may manifest in greater muscle remodeling, a process dependent on the proteasome (24), leading to higher rates of proteasome mediated protein degradation and higher levels of constitutive proteasome components (α7 levels), as seen in the basalt new derivative species (Fig. 4*B*). High proteasome activity enhances the removal of damaged proteins and thereby improves the quality of the proteome and the maintenance of proteostasis. This may increase longevity (25, 26), and helps the cell to resist oxidative stress (25, 27). High levels of proteasome activity have also been seen in other underground-burrowing animals, such as the naked mole rat. Alternatively, compromised nutrition from low food resources as seen in chalk *Spalax*, which relies on lipid metabolism (Fig. 3), may induce autophagy rather than proteasome-mediated degradation for protein recycling (28) (Fig. 4*C*).

Conclusions and Prospects

During SS, natural selection and natural genetic engineering (29) are nonrandomly diverging 317 soil-biased genes, gene networks, and functional structures involved in the whole genome and proteome, coping with local ecologically, differentially, diverse biological stresses (Fig. 3 and Tables S2 and S3). Because the soil populations are abutting, animals can migrate in both directions (4) (Fig. 2*B*), yet philopatry or habitat choice restricts gene flow. Natural selection and natural genetic engineering overrule gene flow, as in Evolution Canyon (6), selecting for soil-specific adaptive complexes and generating adaptive ecological incipient SS. Unfolding the regulatory function of the repeatome, and epigenomics could highlight the SS procession in sharply divergent ecologies, which may occur frequently in nature (1) across sharply divergent geological, climatic, edaphic, and biotic abutting contrasts (6). Basalt populations have more SGs, which may involve genes explained by the niche release hypothesis (30). The *Spalax* example of SS supported by genome-wide adaptive

divergence is one of the few cases (*SI Appendix*) substantiating the occurrence and genetic patterns of SS in nature. Future studies could involve transcriptomes, repeatomes, metabolomics, editomes, and phenomics aspects of the ancestral chalk and derivative basalt populations.

Materials and Methods

All experiments on the blind mole rats were approved by the Ethics Committee of University of Haifa and Wuhan University, and conformed to the rules and guidelines on animal experimentation in Israel and China. Whole genome resequencing of two soil populations of *S. galili*, the ancestral chalk and derivative basalt populations, was performed. Genome-wide divergence between the two mole rat soil populations was estimated by PCA, neighbor-joining phylogenetic tree, and individual ancestry estimation based on the full maximum likelihood method. Genomic characterization of the two soil populations was revealed by differently enriched GO terms, protein proteostasis, olfactory, and bitter taste receptor gene analyses. Genetic diversity and LD of the two soil populations were compared and contrasted. Population demography, effective population size, and gene flow were estimated to assess the evolutionary divergence of sympatric speciation. Population divergent time was estimated by both mitochondrial and nuclear genome analyses. Full details of the materials and methods are described in *SI Materials and Methods*.

ACKNOWLEDGMENTS. We thank Professor Alan R. Templeton and Matěj Lövy for valuable comments and Shay Zur for his photograph. The Major Research Plan of the National Natural Science Foundation of China (91331115) and the Ancell-Teicher Research Foundation for Genetics and Molecular Evolution financially supported this work.

1. Darwin C (1859) *On the Origins of Species by Means of Natural Selection* (John Murray, London).
2. Coyne JA, Orr HA (2004) *Speciation* (Sinauer Associates, Sunderland, MA).
3. Gavrilets S (2004) *Fitness Landscapes and the Origin of Species (MPB-41)* (Princeton Univ Press, Princeton).
4. Hadid Y, et al. (2013) Possible incipient sympatric ecological speciation in blind mole rats (*Spalax*). *Proc Natl Acad Sci USA* 110(7):2587–2592.
5. Hadid Y, et al. (2014) Sympatric incipient speciation of spiny mice *Acomys* at "Evolution Canyon," Israel. *Proc Natl Acad Sci USA* 111(3):1043–1048.
6. Nevo E (2014) Evolution in action: Adaptation and incipient sympatric speciation with gene flow across life at "Evolution Canyon", Israel. *Isr J Ecol Evol* 60(2-4):85–98.
7. Michel AP, et al. (2010) Widespread genomic divergence during sympatric speciation. *Proc Natl Acad Sci USA* 107(21):9724–9729.
8. Fang X, et al. (2014) Genome-wide adaptive complexes to underground stresses in blind mole rats *Spalax*. *Nat Commun* 5:3966.
9. Nevo E (1999) *Mosaic Evolution of Subterranean Mammals: Regression, Progression, and Global Convergence* (Oxford University Press, Oxford, UK).
10. Nevo E (1998) Molecular evolution and ecological stress at global, regional and local scales: The Israeli perspective. *J Exp Zool* 282(1-2):95–119.
11. Polyakov A, Beharav A, Avivi A, Nevo E (2004) Mammalian microevolution in action: Adaptive edaphic genomic divergence in blind subterranean mole-rats. *Proc Biol Sci* 271(Suppl 4):S156–S159.
12. Reich DE, et al. (2001) Linkage disequilibrium in the human genome. *Nature* 411(6834): 199–204.
13. Franssen SU, Nolte V, Tobler R, Schlötterer C (2015) Patterns of linkage disequilibrium and long range hitchhiking in evolving experimental *Drosophila melanogaster* populations. *Mol Biol Evol* 32(2):495–509.
14. Lövy M, et al. (2015) Habitat and burrow system characteristics of the blind mole rat *Spalax galili* in an area of supposed sympatric speciation. *PLoS One* 10(7):e0133157.
15. Smukowski CS, Noor MA (2011) Recombination rate variation in closely related species. *Heredity (Edinb)* 107(6):496–508.
16. Nevo E, Shkolnik A (1974) Adaptive metabolic variation of chromosome forms in mole rats, *Spalax*. *Experientia* 30(7):724–726.
17. Heth G, et al. (1992) Differential olfactory perception of enantiomeric compounds by blind subterranean mole rats (*Spalax ehrenbergi*). *Experientia* 48(9):897–902.
18. Heth G, Todrank J, Nevo E (2000) Do *Spalax ehrenbergi* blind mole rats use food odours in searching for and selecting food? *Ethol Ecol Evol* 12(1):75–82.
19. Li M, et al. (2013) Genomic analyses identify distinct patterns of selection in domesticated pigs and Tibetan wild boars. *Nat Genet* 45(12):1431–1438.
20. Schrader L, et al. (2014) Transposable element islands facilitate adaptation to novel environments in an invasive species. *Nat Commun* 5:5495.
21. Nevo E, Filippucci MG, Beiles A (1994) Genetic polymorphisms in subterranean mammals (*Spalax ehrenbergi* superspecies) in the near east revisited: Patterns and theory. *Heredity (Edinb)* 72(Pt 5):465–487.
22. Nevo E, Pirlot P, Beiles A (1988) Brain size diversity in adaptation and speciation of subterranean mole rats. *J Zoological Syst Evol Res* 26(6):467–479.
23. Smadja C, Butlin RK (2009) On the scent of speciation: The chemosensory system and its role in premating isolation. *Heredity* 102(1):77–97.
24. Rodriguez KA, Edrey YH, Osmulski P, Gaczynska M, Buffenstein R (2012) Altered composition of liver proteasome assemblies contributes to enhanced proteasome activity in the exceptionally long-lived naked mole-rat. *PLoS One* 7(5):e35890.
25. Rodriguez KA, et al. (2011) Walking the oxidative stress tightrope: A perspective from the naked mole-rat, the longest-living rodent. *Curr Pharm Des* 17(22):2290–2307.
26. Chondrogianni N, Georgila K, Kourtis N, Tavernarakis N, Gonos ES (2015) 20S proteasome activation promotes life span extension and resistance to proteotoxicity in *Caenorhabditis* elegans. *FASEB J* 29(2):611–622.
27. Pickering AM, Davies KJ (2012) Degradation of damaged proteins: The main function of the 20S proteasome. *Prog Mol Biol Transl Sci* 109:227–248.
28. Lin T-C, et al. (2012) Autophagy: Resetting glutamine-dependent metabolism and oxygen consumption. *Autophagy* 8(10):1477–1493.
29. Shapiro JA (2011) *Evolution: A View From the 21st Century* (Pearson Education, FT Press Science, Upper Saddle River, NJ).
30. Wu C-I, Ting C-T (2004) Genes and speciation. *Nat Rv Genet* 5(2):114–122.
31. Levitte D (2001) *Geological Map of Israel, 1: 50,000 Sheet 2–III, Zefat* (Geological Survey of Israel, Jerusalem).
32. Nevo E, Ivanitskaya EN, Beiles A (2001) *Adaptive Radiation of Blind Subterranean Mole Rats: Naming and Revisiting the Four Sibling Species of the Spalax ehrenbergi Superspecies in Israel: Spalax galili (2n=52), S. golani (2n=54), S. carmeli (2n=58), and S. judaei (2n=60)* (Backhuys Publishers, Leiden).
33. Li H, Durbin R (2009) Fast and accurate short read alignment with Burrows-Wheeler transform. *Bioinformatics* 25(14):1754–1760.
34. Li H, et al.; 1000 Genome Project Data Processing Subgroup (2009) The sequence alignment/map format and SAMtools. *Bioinformatics* 25(16):2078–2079.
35. Menozzi P, Piazza A, Cavalli-Sforza L (1978) Synthetic maps of human gene frequencies in Europeans. *Science* 201(4358):786–792.
36. Bryc K, et al. (2010) Genome-wide patterns of population structure and admixture in West Africans and African Americans. *Proc Natl Acad Sci USA* 107(2):786–791.
37. Liu Y, et al. (2013) Softwares and methods for estimating genetic ancestry in human populations. *Hum Genomics* 7(1):1.
38. Purcell S, et al. (2007) PLINK: A tool set for whole-genome association and population-based linkage analyses. *Am J Hum Genet* 81(3):559–575.
39. Yang J, Lee SH, Goddard ME, Visscher PM (2011) GCTA: A tool for genome-wide complex trait analysis. *Am J Hum Genet* 88(1):76–82.
40. Tang H, Peng J, Wang P, Risch NJ (2005) Estimation of individual admixture: analytical and study design considerations. *Genet Epidemiol* 28(4):289–301.
41. Saitou N, Nei M (1987) The neighbor-joining method: A new method for reconstructing phylogenetic trees. *Mol Biol Evol* 4(4):406–425.
42. Browning SR, Browning BL (2007) Rapid and accurate haplotype phasing and missing-data inference for whole-genome association studies by use of localized haplotype clustering. *Am J Hum Genet* 81(5):1084–1097.
43. Team RDC (2010) *R: A Language and Environment for Statistical Computing* (R Foundation for Statistical Computing, Vienna).
44. Watterson GA (1975) On the number of segregating sites in genetical models without recombination. *Theor Popul Biol* 7(2):256–276.
45. Auton A, McVean G (2007) Recombination rate estimation in the presence of hotspots. *Genome Res* 17(8):1219–1227.
46. Gronau I, Hubisz MJ, Gulko B, Danko CG, Siepel A (2011) Bayesian inference of ancient human demography from individual genome sequences. *Nat Genet* 43(10): 1031–1034.
47. Rambaut A, Suchard M, Xie D, Drummond A (2014) Tracer v1. 6. Computer program and documentation distributed by the author. Available at beast.bio.ed.ac.uk/Tracer. Accessed July 27, 2014.
48. Gibbs RA, et al. (2004) Genome sequence of the Brown Norway rat yields insights into mammalian evolution. *Nature* 428(6982):493–521.
49. Adkins RM, Walton AH, Honeycutt RL (2003) Higher-level systematics of rodents and divergence time estimates based on two congruent nuclear genes. *Mol Phylogenet Evol* 26(3):409–420.
50. Shanas U, Heth G, Nevo E, Shalgi R, Terkel J (1995) Reproductive behaviour in the female blind mole rat (*Spalax ehrenbergi*). *J Zool (Lond)* 237(2):195–210.
51. Drummond AJ, Rambaut A (2007) BEAST: Bayesian evolutionary analysis by sampling trees. *BMC Evol Biol* 7(1):214.
52. Tajima F (1989) Statistical method for testing the neutral mutation hypothesis by DNA polymorphism. *Genetics* 123(3):585–595.
53. Weir BS, Cockerham CC (1984) Estimating F-statistics for the analysis of population structure. *Evolution* 38(6):1358–1370.
54. Dennis G, Jr, et al. (2003) DAVID: Database for annotation, visualization, and integrated discovery. *Genome Biol* 4(5):3.
55. Yarmolinsky DA, Zuker CS, Ryba NJ (2009) Common sense about taste: From mammals to insects. *Cell* 139(2):234–244.
56. Tamura K, Stecher G, Peterson D, Filipski A, Kumar S (2013) MEGA6: Molecular evolutionary genetics analysis version 6.0. *Mol Biol Evol* 30(12):2725–2729.
57. Librado P, Rozas J (2009) DnaSP v5: A software for comprehensive analysis of DNA polymorphism data. *Bioinformatics* 25(11):1451–1452.
58. Hudson RR (2000) A new statistic for detecting genetic differentiation. *Genetics* 155(4):2011–2014.
59. Liu C-W, et al. (2006) ATP binding and ATP hydrolysis play distinct roles in the function of 26S proteasome. *Mol cell* 24(1):39–50.
60. Rodriguez KA, Gaczynska M, Osmulski PA (2010) Molecular mechanisms of proteasome plasticity in aging. *Mech Ageing Dev* 131(2):144–155.